

---

# Direct Acquisition Optimization for Low-Budget Active Learning

---

Zhuokai Zhao<sup>1</sup> Yibo Jiang<sup>1</sup> Yuxin Chen<sup>1</sup>

## Abstract

Active Learning (AL) has gained prominence in integrating data-intensive machine learning (ML) models into domains with limited labeled data. However, its effectiveness diminishes significantly when the labeling budget is low. In this paper, we first empirically observe the performance degradation of existing AL algorithms in the low-budget settings, and then introduce *Direct Acquisition Optimization* (DAO), a novel AL algorithm that optimizes sample selections based on expected true loss reduction. Specifically, DAO utilizes influence functions to update model parameters and incorporates an additional acquisition strategy to mitigate bias in loss estimation. This approach facilitates a more accurate estimation of the overall error reduction, without extensive computations or reliance on labeled data. Experiments demonstrate DAO’s effectiveness in low budget settings, outperforming state-of-the-arts approaches across seven benchmarks.

## 1 Introduction

Active learning (AL) explores how adaptive data collection can reduce the amount of data needed by machine learning (ML) models (Settles, 2009; Ren et al., 2021). It is particularly useful when labeled data is scarce or expensive to obtain, which significantly limits the adaptability of modern deep learning (DL) models due to their data-hungry nature (van der Ploeg et al., 2014). In these cases, AL algorithms selectively choose the most beneficial data points for labeling, thereby maximizing the effectiveness of the training process even if the data is limited in number. In fact, AL has been broadly applied in many fields (Adadi, 2021), such as medical image analysis (Budd et al., 2021), astronomy (Škoda et al., 2020), and physics (Ding et al., 2023), where unlabeled samples are plentiful but the process of labeling through human expert annotations or experiments is highly cost-intensive. In these contexts, judiciously select-

ing samples for labeling can significantly lower the expenses involved in compiling the datasets (Ren et al., 2021).

Many active learning algorithms have emerged over the past decades, with early seminal contributions from (Lewis, 1995; Tong & Koller, 2001; Roy & McCallum, 2001), and a shift that focuses more on deep active learning - a branch of AL that targets more towards DL models in more recent years (Huang, 2021). Depending on the optimization objective, AL algorithms can be classified into two categories. The first category includes heuristic objectives that are not exactly the same as the evaluation metric, i.e. error reduction. Examples in this category are diversity (Sener & Savarese, 2017), uncertainty (Gal et al., 2017), and hybrids of both (Ash et al., 2019). Second category includes criteria that is exactly the same as the evaluation metric, where notable approaches include expected error reduction (EER) (Roy & McCallum, 2001) and its modern follow-up works (Killamsetty et al., 2021; Musmann et al., 2022).

Despite the popularity of the first type of AL algorithms, we show in §2 that these methods often suffer heavily in low-budget settings, where the total (accumulative) sampling quota is less than 1% of the number of unlabeled data points, making them less suitable for the extreme data scarcity scenarios. In terms of the methods from the second category, their higher running time and reliance on the availability of a *validation* or *hold-out* set remain significant limitations, constraining their applicability in many data-scarcity scenarios as well. For example, EER (Roy & McCallum, 2001) re-trains the classifier for each candidate with all its possible labels, where in each time also evaluates the updated model on all the unlabeled data, making its runtime intractable especially for deep neural networks. And GLISTER (Killamsetty et al., 2021), despite being much more computationally efficient, requires a *labeled, hold-out* set for its sample selection process, formulated as a mixed discrete-continuous bi-level optimization problem, to be optimized properly.

While these constraints might not be a huge limitation a few years ago, it poses a more important challenge currently as we are adopting deep learning models to more areas, where labeled data may be extremely expensive to acquire. More importantly, it is also worth noticing that under these scenarios, the highly limited labeled data should have been better

---

<sup>1</sup>Department of Computer Science, University of Chicago, Chicago IL, USA. Correspondence to: Zhuokai Zhao <zhuokai@uchicago.edu>.

utilized for training than being reserved for AL algorithms.

Above limitations highlight a critical gap between the capabilities of current AL methodologies and the urgent demands from real-world applications, underscoring the need for developing novel AL strategies that can operate both relatively efficient while presenting little to none reliance on the labeled set. To this end, we introduce **Direct Acquisition Optimization (DAO)**, a novel AL algorithm that selects new samples for labeling by efficiently estimating the expected loss reduction. Compared to EER and GLISTER, DAO solves the pain points of prohibitive running time and the reliance on a separate labeled set through utilizing *influence function* (Ling, 1984) in model parameters updates, and a more accurate, efficient unbiased estimator of loss reduction through importance-weighted sampling.

To summarize, the contributions of this paper are: (1) an empirical analysis of existing AL algorithms under low budget settings; (2) a novel AL algorithm, Direct Acquisition Optimization (DAO), which optimizes sample selections based on expected error reduction while operating efficiently through influence function-based model parameters approximation and true overall reduced error estimation; and (3) thorough experiments demonstrating DAO’s superior performance in the low-budget settings, out-performing current popular AL methods across seven benchmarks.

## 2 Low-Budget Active Learning: A Motivating Case Study

In this section, we provide an empirical analysis to demonstrate that commonly used heuristic-based AL algorithms do not work well under very low-budget settings. Specifically, we analyze (1) uncertainty sampling methods including least confidence (Lewis, 1995), minimum margin (Scheffer et al., 2001), maximum entropy (Settles, 2009), and Bayesian Active Learning by Disagreement (BALD) (Gal et al., 2017); (2) diversity sampling methods such as Core-Set (Sener & Savarese, 2017) and Variational Adversarial Active Learning (VAAL) (Sinha et al., 2019); and (3) hybrid method such as Batch Active learning by Diverse Gradient Embeddings (BADGE) (Ash et al., 2019).

We test the above methods on the CIFAR10 (Krizhevsky et al., 2009) dataset starting with an initial labeled set with size  $|\mathcal{L}_{\text{init}}| = 10$ , and conducted 50 acquisition rounds where after each round  $B = 10$  new samples are selected and labeled. We use ResNet-18 (He et al., 2016) as our training model across all methods. And we repeated the acquisitions five times with different random seeds. The results are visualized in Fig. 1, where we plot the *relative* performance between each method and random sampling acquisition through a diverging color map.

Aligning with the general perceptions that low-budget (Mit-

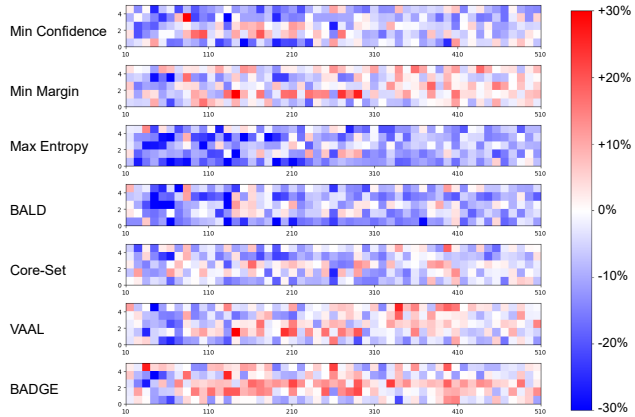


Figure 1. Existing methods fail to outperform random sampling with small budgets. This figure shows the relative performance between multiple methods and random acquisition. Within each subplot,  $x$  axis represents the accumulative acquisition size, while  $y$  axis indicates runs initiated with different random seeds. White color indicates on-par performance with random, blue indicates worse, and red indicates better.

tal et al., 2019; Hacoheh et al., 2022) and cold-start (Zhu et al., 2019; Chandra et al., 2021) AL tasks are especially challenging, we empirically observe that almost all popular AL algorithms fail to outperform the naive random sampling when acquisition quota is less than 1% (500 out of 50,000 in the case of CIFAR10) of the unlabeled size. More specifically, when the quota is less than 0.2% (less than 100 data points for CIFAR-10), all methods fail to reliably outperform random sampling (as the beginning of each heatmap in Fig. 1 are almost all blue), which greatly motivates the development of DAO. We also include the more conventional line plot of the empirical analysis which may provide more detailed information of each run in Appendix A.1.

## 3 Methodology

Different from the heuristics-based AL algorithms that optimize criteria such as diversity or uncertainty, DAO is built upon the EER formulation with the selection objective being the largest reduced error evaluated on the entire unlabeled set. More specifically, DAO majorly improves upon two aspects: (1) instead of re-training the classifier, we employ influence function (Cook & Weisberg, 1982), a concept with rich history in statistical learning, to formulate the new candidate sample as a small perturbation to the existing labeled set, so that the model parameters can be estimated without re-training; and (2) instead of reserving a separate, relatively large labeled set for validation (Killamsetty et al., 2021), we sample a very small subset directly from the *unlabeled* set and estimate the loss reduction through bias correction.

Essentially, when considering each candidate from the unlabeled set, we optimize the EER framework on two of its core components, which are model parameter update and

true loss estimation. Additionally, we upgrade EER, which only supports single sequential acquisition, to offer DAO in both single and batch acquisition variants by incorporating stochastic samplings to the sorted estimated loss reductions. We illustrate our algorithmic framework in Fig. 2. In the following parts of this section, we first introduce a more formal problem statement in §3.1, and then dive into each specific component of DAO from §3.2 to §3.5.

### 3.1 Problem Statement

The optimal sequential active learning acquisition function can be formulated as selecting a single  $\mathbf{x}_t^{\text{train}}$  from the current unlabeled set  $\mathcal{U}_t$  at each round  $t$  such that

$$\mathbf{x}_t^{\text{train}} = \arg \min_{\mathbf{x}_i \in \mathcal{U}_{t-1}} \mathbb{E}_{(y_i | f^*, \mathbf{x}_i)} [L_{\text{true}}(f_{t|\mathbf{x}_i, y_i})] \quad (1)$$

where  $f^*$  represents an optimal oracle that maps from any unlabeled data  $\mathbf{x}_i \in \mathcal{U}_{t-1}$  to its ground-truth label  $y_i$ , and  $f_{t|\mathbf{x}_i, y_i}$  is the model that has been trained on the union of the current labeled set  $\mathcal{L}_{t-1}$  and the current unlabeled candidate  $\mathbf{x}_i \in \mathcal{U}_{t-1}$ . In addition,  $L_{\text{true}}(f_{t|\mathbf{x}_i, y_i}) = \frac{1}{|\mathcal{U}_{t-1, i}|} \sum_{\mathbf{x} \in \mathcal{U}_{t-1, i}} \ell(\mathbf{x}; f_{t|\mathbf{x}_i, y_i})$  represents the loss estimator that can predict the *unbiased* error of  $f_{t|\mathbf{x}_i, y_i}$ , where  $\ell$  denotes the loss of  $f_{t|\mathbf{x}_i, y_i}$  evaluated on  $\mathbf{x}_i$  (against its true label  $f^*(\mathbf{x}_i)$ ). It is numerically the same as if  $f_{t|\mathbf{x}_i, y_i}$  has been tested on the entire unlabeled set  $\mathcal{U}_{t-1, i}$ , where  $\mathcal{U}_{t-1, i} = \mathcal{U}_{t-1} \setminus \{\mathbf{x}_i\}$ . Such formulation represents the optimal AL algorithm and aligns with any existing sequential active learning algorithm — of which the goal is to select the new data point that can most significantly improve the current model performance (Roy & McCallum, 2001).

Unfortunately, Eq. (1) cannot be directly implemented in practice. Because, first, we do not have access to the optimal oracle  $f^*$  to reveal the label  $y_i$  for each  $\mathbf{x}_i \in \mathcal{U}_{t-1}$ ; second, even if we had  $f^*$  and therefore  $y_i$ , we cannot afford the cost of retraining model  $f_{t-1}$  on each  $\mathcal{L}_{t-1} \cup \mathbf{x}_i$  to obtain the updated  $f_{t|\mathbf{x}_i, y_i}$ ; and third, we do not have the unbiased true loss estimator  $L_{\text{true}}$ , which demands evaluating  $f_{t|\mathbf{x}_i, y_i}$  on the entire  $\mathcal{U}_{t-1, i}$ .

Therefore, the goal of DAO is to solve the above challenges and efficiently and accurately approximate Eq. (1) for the sample selection strategy. It is also worth noting that, when  $\mathbf{x}_t^{\text{train}}$  represents a *set* of newly acquired data points, the above formulation becomes eligible for batch active learning, which is more suitable for deep neural networks (Huang, 2021).

### 3.2 Label Approximation via Surrogate

In this section, we address the first challenge when approximating Eq. (1). As we do not know the true label or true label distribution  $p(y|\mathbf{x}, f^*)$  of each unlabeled sample  $\mathbf{x}$ , the best we can do is provide an approximation for  $p(y|\mathbf{x})$ . To this end, we introduce the concept of a *surrogate*

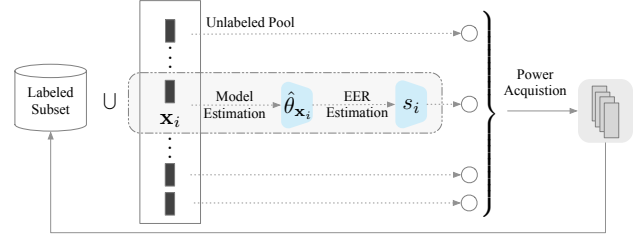


Figure 2. Schematic of the algorithmic framework of DAO.

*gate* (Kossen et al., 2021), which is a model parameterized by some potentially infinite set of parameters  $\theta$ . Specifically,  $p(y|\mathbf{x})$  can be approximated using the marginal distribution  $\pi(y|\mathbf{x}) = \mathbb{E}_{\pi(\theta)}[\pi(y|\mathbf{x}, \theta)]$  with some proposal distribution  $\pi(\theta)$  over model parameters  $\theta$ . In other words, we have:

$$p(y|\mathbf{x}) \approx \int_{\theta} \pi(\theta) \pi(y|\mathbf{x}, \theta) d\theta \quad (2)$$

As the sample selection process continues, new labeled points should also be used to train and update the surrogate model  $\pi(\theta)$  for better approximation of the true outcomes.

Although ideally, a more capable surrogate is preferred for better ground truth approximations, we acknowledge that the choice of surrogate model can be very sensitive to the computational constraints. Therefore, if running time is at center of the concerns during sample acquisitions, using  $f_t$  at step  $t$  also as the surrogate could be an efficient alternative, as we don't need to update a second model, nor do we need to run forward pass on the both models. However, this will come with the cost that  $\pi_t$  never disagrees with  $f_t$ , which causes performance degradation for the unbiased true loss estimation, which will be illustrated with more details in §3.4. Therefore, in short, we do not recommend replicating  $f_t$  as surrogate in practice, unless the computational constraint is substantial.

### 3.3 Model Parameters Update without Re-training

At acquisition round  $t$ , suppose we have labeled set  $\mathcal{L}_{t-1}$  and unlabeled set  $\mathcal{U}_{t-1}$  as the results from the previous round  $t-1$ , and new sample  $\mathbf{x}_i \in \mathcal{U}_{t-1}$  that is currently under consideration for acquisition, the goal of this section is to estimate the parameters of model  $f_{t|\mathbf{x}_i, y_i}$  that could have been obtained after training  $f_{t-1}$  on the combined dataset  $\{\mathcal{L}_{t-1} \cup \mathbf{x}_i\}$ . In other words, if we suppose the conventional full training converges to parameters  $\hat{\theta}_{\mathbf{x}_i}$ , we have:

$$\hat{\theta}_{\mathbf{x}_i} = \arg \min_{\theta \in \Theta} \frac{1}{|\mathcal{L}_{t-1}| + 1} \sum_{\mathbf{x} \in \{\mathcal{L}_{t-1} \cup \mathbf{x}_i\}} \ell(\mathbf{x}; \theta) \quad (3)$$

where recall that  $\ell(\mathbf{x}; \theta)$  denotes the loss of  $\theta$  on  $\mathbf{x}$ . The core of our approach is that, instead of re-training as showed in Eq. (3), we can approximate the effect of adding a new sample as upweighting the influence function by  $\frac{1}{|\mathcal{L}_{t-1}| + 1}$  (Koh

& Liang, 2017) and then directly estimate the updated model parameters.

Following (Cook & Weisberg, 1982), we have the influence function defined as:

$$\mathcal{I}_{\text{up,params}}(\mathbf{x}_i) := \left. \frac{d\hat{\theta}_{\epsilon,\mathbf{x}_i}}{d\epsilon} \right|_{\epsilon=0} = -H_{\hat{\theta}}^{-1} \nabla_{\theta} \ell(\mathbf{x}_i; \hat{\theta}) \quad (4)$$

where  $H_{\hat{\theta}}$  is the positive definite Hessian matrix (Koh & Liang, 2017). Next, we can estimate the model parameters after adding this new sample  $\mathbf{x}_i$ , as:

$$\begin{aligned} \hat{\theta}_{\mathbf{x}_i} - \hat{\theta} &\approx \frac{1}{|\mathcal{L}_{t-1}| + 1} \mathcal{I}_{\text{up,params}}(\mathbf{x}_i) \\ &= -\frac{1}{|\mathcal{L}_{t-1}| + 1} H_{\hat{\theta}}^{-1} \nabla_{\theta} \ell(\mathbf{x}_i; \hat{\theta}) \end{aligned} \quad (5)$$

where  $\nabla_{\theta} \ell(\mathbf{x}_i; \hat{\theta})$  could be approximated as the expected gradient of sample  $\mathbf{x}_i$ : By a slight abuse of notation of the training loss function  $\ell$ , we denote

$$\nabla_{\theta} \ell(\mathbf{x}_i; \hat{\theta}) \approx \sum_{k=1}^K \nabla_{\theta} \ell(\mathbf{x}_i, \hat{y}_k; \hat{\theta}) \cdot \hat{p}_k \quad (6)$$

In Eq. (6),  $\hat{y}_k$  and  $\hat{p}_k$  represent model’s label prediction and likelihood (e.g. confidence) respectively while  $K$  represents the total number of classes in the ground truths.

In practice, the inverse of  $H_{\hat{\theta}}$  cannot be computed due to its prohibitive  $O(np^2 + p^3)$  runtime (Liu et al., 2021), with  $p$  being the number of model parameters. The computation unavoidably becomes especially intensive when  $f$  is a deep neural network model (Fu et al., 2018). Luckily, we have two optimization methods, conjugate gradients (CG) (Martens et al., 2010) and stochastic estimation (Agarwal et al., 2017) at our disposal.

**Conjugate gradients.** As mentioned earlier, by assumption we have  $H_{\hat{\theta}} \succ 0$  and  $\nabla_{\theta} \ell(\mathbf{x}'; \hat{\theta})$  as a vector. Therefore, we can calculate the inverse Hessian vector product (IHVP) through first transforming the matrix inverse into an optimization problem, i.e.

$$H_{\hat{\theta}}^{-1} \nabla_{\theta} \ell(\mathbf{x}_i; \hat{\theta}) \equiv \arg \min_t t^T H_{\hat{\theta}} t - v^T t \quad (7)$$

and then solving it with CG (Martens et al., 2010), which speeds up the runtime effectively to  $O(np)$ .

**Stochastic estimation.** Besides CG, we can also efficiently compute the IHVP using the stochastic estimation algorithm developed by Agarwal et al. (Agarwal et al., 2017). From Neumann series, we have  $A^{-1} \approx \sum_{i=0}^{\infty} (I - A)^i$  for any matrix  $A$ . Similarly, suppose we define the first  $j$  terms in the Taylor expansion of  $H_{\hat{\theta}}^{-1}$  as

$$H_{\hat{\theta},j}^{-1} = \sum_{i=0}^j (I - H_{\hat{\theta}})^i = I + (I - H_{\hat{\theta}}) H_{\hat{\theta},j-1}^{-1} \quad (8)$$

we have  $H_{\hat{\theta},j}^{-1} \rightarrow H_{\hat{\theta}}^{-1}$  as  $j \rightarrow \infty$ . The core idea of the stochastic estimation is that the Hessian matrix  $H_{\hat{\theta}}$  can be substituted with any unbiased estimation when computing  $H_{\hat{\theta}}^{-1}$ . In practice, we sample  $n_{\text{ihvp}}$  data points from the existing labeled set  $\mathcal{L}_{t-1}$  and use  $\nabla_{\theta}^2 \ell(\mathbf{x}_i; \hat{\theta})$  as the estimator of  $H_{\hat{\theta}}$  (Liu et al., 2021). Notice that since  $n_{\text{ihvp}}$  is usually very small (in our experiments we used  $n_{\text{ihvp}} = 8$ ), it does not create a constraint on the size of the current labeled set, which does not interfere with the low-budget settings.

Finally, we can approximate the model parameters after the addition of  $\mathbf{x}_i$  as

$$\hat{\theta}_{\mathbf{x}_i} = \hat{\theta} - \frac{1}{n+1} H_{\hat{\theta}}^{-1} \nabla_{\theta} \ell(\mathbf{x}_i; \hat{\theta}) \quad (9)$$

which does not require any re-training. And we will demonstrate in §5.1 that this parameter update strategy provides much better approximations than the naive single backpropagation as seen in the existing AL literature (Killamsetty et al., 2021).

### 3.4 Efficient Unbiased Loss Estimation

Referring back to Eq. (1), the last challenge that we need to address is to gain access to the unbiased true loss estimator  $L_{\text{true}}$ . In other words, we want to predict the *true* performance of  $f_{t|\mathbf{x}_i, y_i}$  on the unlabeled set  $\mathcal{U}_{t,i}$  without exhaustive testing. Strictly, such evaluation cannot be drawn until  $f_{t|\mathbf{x}_i, y_i}$  is evaluated on the entire unlabeled set  $\mathcal{U}_{t,i}$ . However, this is infeasible in practice.

Such approximation is typically carried out in other approaches (Killamsetty et al., 2021; Musmann et al., 2022) by randomly sampling a labeled validation set  $\mathcal{V}$  at the beginning of the entire acquisition process, which will later be used for evaluations in all the subsequent acquisition episodes. Despite the simplicity as well as being i.i.d., which makes the estimated loss unbiased by nature, this approximation method suffers from large variance as the size of  $\mathcal{V}$  is usually much smaller than  $\mathcal{U}$ , which unavoidably hurts the acquisition performance. It is also contradictory to the goal of AL in general, especially under the low-budget settings, as discussed in §1.

Different from the existing works, we propose to sample a subset  $\mathcal{C}$  from current  $\mathcal{L}_{t-1}$  in each acquisition round based on an alternative acquisition function, and then correct the bias in the loss induced from this acquisition function. In the meantime, we also want to keep the variance low, so that the final corrected loss enjoys both low bias and low variance, which is more preferable than the zero bias but high variance that the random i.i.d. sampling has.

Specifically, continuing with the notations from §3.1, let  $\mathcal{C} = \{\mathbf{x}_{t,1}, \dots, \mathbf{x}_{t,m}, \dots, \mathbf{x}_{t,n_{\mathcal{C}}}\}$ , where  $\mathcal{C} \subset \mathcal{U}_{t-1}$ , be the subset containing  $n_{\mathcal{C}}$  samples selected for this true loss estimation at each round  $t$ . Farquhar et al. (2021) shows

that if  $\mathbf{x}_{t,m}$  is sampled in proportion to the true loss of each data point, the bias originated from this selection can be corrected through the Monte Carlo estimator  $\hat{R}_{\text{LURE}}^1$ . Following our notations, it takes the form:

$$\hat{R}_{\text{LURE}} = \frac{1}{n_{\mathcal{C}}} \sum_{m=1}^{n_{\mathcal{C}}} v_m \ell(\mathbf{x}_{t,m}; f) \quad (10)$$

where recall that  $\ell$  denotes the loss of  $f$ , and the importance weight  $v_m$  is

$$v_m = 1 + \frac{|\mathcal{U}_{t-1}| - n_{\mathcal{C}}}{|\mathcal{U}_{t-1}| - m} \left( \frac{1}{(|\mathcal{U}_{t-1}| - m + 1)q_t^*(m)} - 1 \right) \quad (11)$$

with  $q_t^*(m)$  being the acquisition distribution of index  $m$  at round  $t$ . Importantly, the variance can be significantly reduced if the acquisition distribution  $q_t^*(m)$  is proportion to the true loss of each data point. Again, this is not feasible as we do not have access to the labels for  $\mathcal{U}_{t-1}$ . However, following Kossen et al. (2021), we can approximate  $q_t^*(m)$  with

$$q_t(m) = - \sum_y \pi(y|\mathbf{x}_{t,m}) \log f(\mathbf{x}_{t,m}) \quad (12)$$

for classification tasks when the loss function is the cross-entropy loss, and where  $\pi$  is conveniently just our surrogate discussed in §3.2. Referring back to the discussion we had on choosing a good surrogate  $\pi$ , with  $f(\mathbf{x})$  being designed to approximate  $p(y|\mathbf{x})$  as well, the surrogate  $\pi$  should ideally be different from  $f$  so that more diversity is introduced in the acquisitions.

To put all the components together, our loss correction process involves selecting samples in  $\mathcal{C}$  based on

$$\mathbf{x}_{t,m} \propto - \sum_y \pi_{t-1}(y|\mathbf{x}) \log f_{t-1}(y|\mathbf{x}) \quad (13)$$

where  $\pi_{t-1}$  is the surrogate model  $\pi$  at round  $t-1$ . Finally, the corrected loss  $s_i$  can be approximated using  $\hat{R}_{\text{LURE}}$  as

$$s_i = \frac{1}{n_{\mathcal{C}}} \sum_{m=1}^{n_{\mathcal{C}}} \hat{v}_m \ell(\mathbf{x}_{t,m}; f_t) \quad (14)$$

where  $\hat{v}_m$ , which depends on the choice of  $\mathbf{x}_{t,m}$ , is the approximated version of the original  $v_m$  defined in Eq. (11). Specifically,  $\hat{v}_m$  takes the form

$$\hat{v}_m = 1 + \frac{|\mathcal{U}_{t-1}| - n_{\mathcal{C}}}{|\mathcal{U}_{t-1}| - m} \left( \frac{1}{(|\mathcal{U}_{t-1}| - m + 1)q_t(m)} - 1 \right) \quad (15)$$

where  $q_t(m)$  is the acquisition function defined in Eq. (13).

### 3.5 Batch Acquisition via Stochastic Sampling

In §3.1, we briefly discussed that when  $\mathbf{x}_t^{\text{train}}$  represents a set of data points (instead of a single one), the formulation

in Eq. (1) essentially represents the *batch* active learning scenario. Suppose the acquisition budget per round is  $k$ , although selecting the top  $k$  samples with the lowest estimated losses (or highest expected error reduction) is straightforward, this approach is sub-optimal. This is because top- $k$  acquisition, while effective to some degree due to its greedy nature, overlooks the crucial interactions among data points in batch acquisitions. Specifically, while aiming to select the most informative unlabeled points, top- $k$  acquisition may lead to redundant choices, diminishing the overall benefit of the acquisition.

Inspired by Kirsch et al. (2021), we propose to similarly perturb the original ranking of the estimated true losses so that the batch sampling provides better acquisitions when the most informative data points may be duplicated. Suppose at acquisition episode  $t$ , we rank the set of estimated true loss of each unlabeled data point in ascending orders as  $\{\hat{l}_{\text{true},i}\}_{\mathbf{x}_i \in \mathcal{U}_{t-1}}$ , such that  $\hat{l}_{\text{true},i} \leq \hat{l}_{\text{true},j}, \forall i \leq j$  and  $\mathbf{x}_i, \mathbf{x}_j \in \mathcal{U}_{t-1}$ , we can perturb the ranking with three strategies: soft-rank, soft-max, and power acquisition, to improve batch performance from the naive top- $k$  sampling.

**Soft-rank acquisition.** Soft-rank acquisition relies on the relative ordering of the scores while ignoring the absolute score values. It samples the data point ranked at index  $i$  with probability  $p_{\text{sofrank}}(i) = i^{-\beta}$ , where  $\beta$  is the ‘‘coldness’’ parameter and is kept as 1 throughout this paper. It is not hard to notice that  $p_{\text{sofrank}}(i)$  is invariant to  $\hat{l}_{\text{true},i}$ , as long as the relative ranking remains the same. More conveniently, with sampled Gumbel noise  $\epsilon_i \sim \text{Gumbel}(0; \beta^{-1})$ , taking the top- $k$  data points from the perturbed ranked list

$$\hat{l}_{\text{true},i}^{\text{sofrank}} = -\log i + \epsilon_i \quad (16)$$

is equivalent to sampling  $p_{\text{sofrank}}(i)$  without replacement (Huijben et al., 2022).

**Soft-max acquisition.** In contrast to soft-rank, soft-max acquisition uses the actual scores, i.e., the estimated true losses, instead of their relative orderings. However, this acquisition does not rely on the semantics of the actual values, resulting in the transformed true loss simply being:

$$\hat{l}_{\text{true},i}^{\text{softmax}} = \hat{l}_{\text{true},i} + \epsilon_i \quad (17)$$

where  $\epsilon_i$  remains the same Gumbel noise as in the soft-rank acquisition. Statistically, choosing the top- $k$  data points from this perturbed ranked list is equivalent to sample from  $p_{\text{softmax}}(i) = e^{\beta i}$  without replacement.

**Power acquisition.** While neither soft-rank or soft-max acquisitions take the semantic meaning of the actual score values into account when designing the acquisition distribution, power acquisition uses the value directly when determining the perturbed values. Specifically, the power acquisition perturbs the scores as

$$\hat{l}_{\text{true},i}^{\text{power}} = \log \hat{l}_{\text{true},i} + \epsilon_i \quad (18)$$

<sup>1</sup>LURE stands for Levelled Unbiased Risk Estimator

---

**Algorithm 1** Direct Acquisition Optimization (DAO)

**input** Episode  $t$ , unlabeled set  $\mathcal{U}_{t-1}$ , labeled set  $\mathcal{L}_{t-1}$ , model  $f_{t-1}$ , surrogate  $\pi_{t-1}$ , budget  $k$ ,  $n_{\text{ihvp}}$  (§3.3), and  $n_C$  (§3.4)  
**output** Acquisition set  $\mathcal{A}_t = \{\mathbf{x}_{t,1}^{\text{train}}, \dots, \mathbf{x}_{t,k}^{\text{train}}\}$  ▷ Eq. (1)  
 1: Approximate  $p(y|\mathbf{x})$  for all  $\mathbf{x} \in \mathcal{U}_{t-1}$  ▷ §3.2, Eq. (2)  
 2: Initialize array  $S$  where  $|S| = |\mathcal{U}_{t-1}|$   
 3: **for**  $i = 1$  **to**  $|\mathcal{U}_{t-1}|$  **do**  
 4:   Let  $\mathcal{U}_{t,i} = \mathcal{U}_{t-1} \setminus \{\mathbf{x}_i\}$   
 5:   Randomly sample  $n_{\text{ihvp}}$  data points from  $\mathcal{U}_{t,i}$   
 6:   Approximate parameters of  $f_{t|\mathbf{x}_i, y_i}$  ▷ §3.3, Eq. (9)  
 7:   Acquire  $n_C$  samples from  $\mathcal{U}_{t,i}$  ▷ §3.4, Eq. (13)  
 8:   Compute  $s_i$  and add to  $S$  ▷ §3.4, Eq. (14)  
 9: **end for**  
 10: Sort  $S$  in ascending order  
 11: **if**  $k > 1$  **then**  
 12:   Perturb  $S$  ▷ Methods showed in §3.5  
 13: **end if**  
 14: Return top- $k$  samples in  $S$  as  $\mathcal{A}_t$

---

where again  $\epsilon_i$  is the Gumbel noise, and choosing the top- $k$  indices from this new list is equivalent to sampling from  $p_{\text{power}}(i) = i^\beta$  without replacement. Results comparing DAO with different batch acquisition strategies discussed above are showed in Appendix A.2.

Combining all the components, the pseudocode of DAO is summarized in Algorithm 1.

## 4 Experiments

We evaluate DAO on seven classification benchmarks including digit recognition datasets MNIST (LeCun et al., 1998), Street-View House Numbers recognition (SVHN) (Sermanet et al., 2012), object classification datasets STL-10 (Coates et al., 2011), CIFAR-10, CIFAR-100 (Krizhevsky et al., 2009), as well as domain-specific datasets Fashion-MNIST (Xiao et al., 2017) and Stanford Cars (Cars196) (Krause et al., 2013).

### 4.1 Experimental Setup

**Baselines.** To ensure fair comparisons, besides baseline methods that we empirically surveyed in §2, we also include other state-of-the-arts AL methods, including Deep Bayesian Active Learning (DBAL) (Gal et al., 2017) and GLISTER (Killamsetty et al., 2021), where GLISTER is a direct competitor that also optimizes the EER framework.

For all the baselines, we used the default/recommended parameters and their official implementations if publicly available. In terms of earlier works such as least confidence (Lewis, 1995), minimum margin (Scheffer et al., 2001), and maximum entropy (Settles, 2009), we used the peer-reviewed deep active learning framework DeepAL+ (Zhan et al., 2022). All experiments are repeated

ten times with different random seeds.

**Implementation details.** Throughout the experiment section, we set ResNet-18 (He et al., 2016) as the model  $f$  to be trained from scratch. We employed VGG16 (Simonyan & Zisserman, 2014), initialized with random weights, as our surrogate  $\pi$ . We used stochastic estimation (Agarwal et al., 2017) when estimating the updated model parameters, as discussed in §3.3. We choose  $n_{\text{ihvp}} = 8$  when approximating the unbiased estimator of  $H_{\hat{\theta}}$ , and set  $n_C = 16$  for biased loss correction as in §3.4.

### 4.2 Digit Recognition

First, we demonstrate DAO’s effectiveness through two digit recognition benchmarks: MNIST (LeCun et al., 1998) and SVHN (Sermanet et al., 2012). MNIST is a collection of handwritten digits consisting of 60k training and 10k test images, while SVHN is a more challenging dataset containing over 600k real-world house numbers images taken from street views. Both datasets contain 10 classes corresponding to digits from 0 to 9.

Based on the insights from §2, we define a general rule of low-budget setting as *one image per class*, which translates to initial label size  $|\mathcal{L}_{\text{init}}^{\text{MNIST}}| = 10$  and per-episode budget  $B_{\text{MNIST}} = 10$  for MNIST. Given that SVHN is more challenging, and there are ten times more unlabeled images than in MNIST (600k vs. 60k), we experiment both  $|\mathcal{L}_{\text{init}}^{\text{SVHN}}| = 10$ ,  $B_{\text{SVHN}} = 10$  and  $|\mathcal{L}_{\text{init}}^{\text{SVHN}}| = 100$ ,  $B_{\text{SVHN}} = 100$  for SVHN. The results are showed in Fig. 3b and 3c.

### 4.3 Object Classification

Next, we assess DAO on more general and complex object classification tasks. STL-10 (Coates et al., 2011) is a benchmark dataset derived from labeled examples in the ImageNet (Deng et al., 2009). Specifically, STL-10 contains 5k labeled  $96 \times 96$  color images spread across 10 classes, as well as 8k images in the test split. CIFAR-10 (Krizhevsky et al., 2009) contains a collection of 60k  $32 \times 32$  color images in 10 different classes, with 6k images per class. CIFAR-100 is similar to CIFAR-10, but covers a much wider range, containing 100 classes where each class holds 600 images.

Continuing with the low-budget setting (*1 image per class*), we have  $|\mathcal{L}_{\text{init}}^{\text{STL-10}}| = 10$ ,  $B_{\text{STL-10}} = 10$  for STL-10,  $|\mathcal{L}_{\text{init}}^{\text{CIFAR-10}}| = 10$ ,  $B_{\text{CIFAR-10}} = 10$  for CIFAR-10 and  $|\mathcal{L}_{\text{init}}^{\text{CIFAR-100}}| = 100$ ,  $B_{\text{CIFAR-100}} = 100$  for CIFAR-100. The results are showed in Fig. 3d, 3e and 3f respectively.

### 4.4 Domain Specific Tasks

The last part of our experiments involves case studies on applying DAO to domain-specific tasks, which simulates many real-world applications. Specifically, we use Fashion-MNIST (Xiao et al., 2017) and StanfordCars (Krause et al., 2013), also known as Cars196, in this experiment. Fashion-

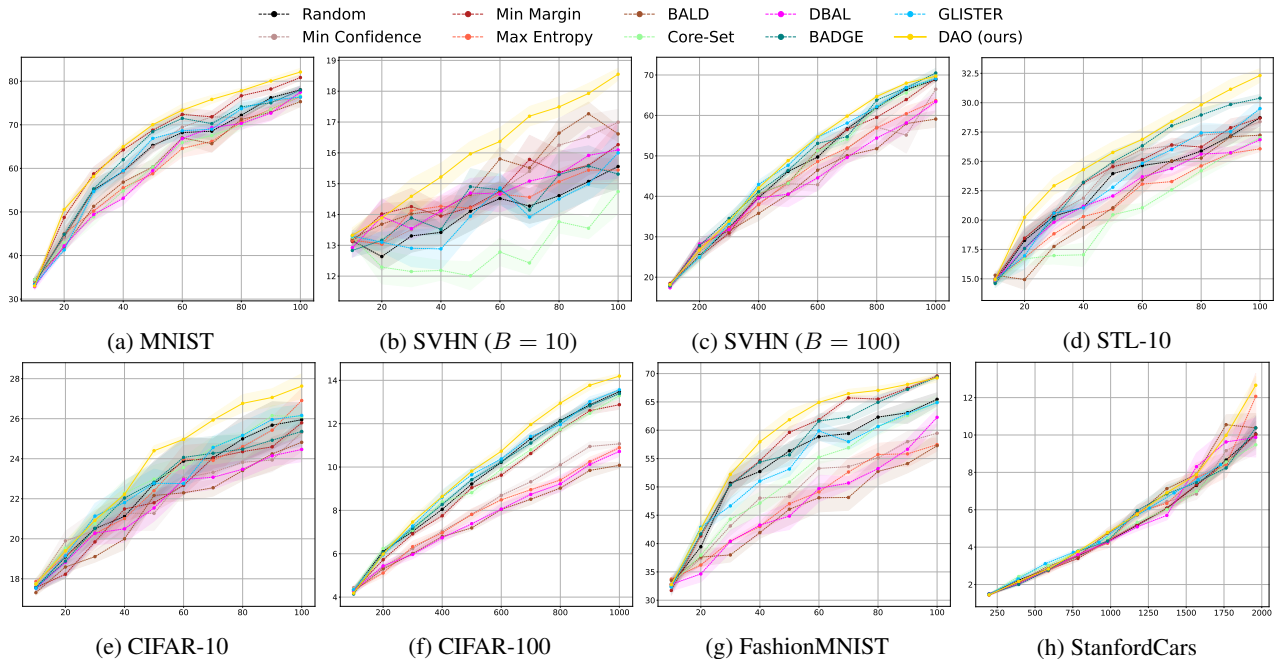


Figure 3. Experiment results comparing DAO with existing AL algorithms across seven benchmarks. In all subplots, horizontal axis represents the accumulative size of the labeled set, while vertical axis indicates classification accuracy.

ionMNIST is structure-wise similar to MNIST, comprising  $28 \times 28$  images of 70k fashion products from 10 categories, with 7k images per category. The training set contains 60k images, while the test set includes the rest. StanfordCars is a large collection of car images, containing 16,185 images with a near-balanced ratio on the train/test split, resulting in 8,144 and 8,041 images for training and testing. There are 196 classes in total, where each class consists of the year, make, model of a car (e.g., 2012 Tesla Model S). The results of both datasets are showed in Fig. 3g and 3h.

#### 4.5 Discussion

From Fig. 3, we notice that the proposed DAO outperforms popular AL state-of-the-arts by a clear margin across all seven benchmarks. Especially, with SVHN, when the budget is extremely low ( $B = 10$ , which is 0.0017% of the unlabeled size), DAO leads the performance by a very large gap, indicating its superior capability in the low-budget setting. Such performance does not degrade much as the budget constraint is relaxed. As shown in Fig. 3c, DAO still performs relatively well. The only experiment that DAO does not improve as much is the StanfordCars. However, the accuracy improvement from DAO is more smooth and has less variance, indicating better robustness when applied to the more challenging (StanfordCars has 196 classes) applications.

### 5 Component Analysis and Ablation Studies

We now analyze specific components of DAO and conduct ablation studies on the strategies proposed for model param-

eters approximation (§5.1) and true loss prediction (§5.2).

#### 5.1 Accuracy on Model Approximation

First, we assess if estimating the model parameters updates through modelling the effect of adding a new sample as upweighting the influence function provides a more accurate model performance approximation than using single backpropagation as seen in the existing work (Killamsetty et al., 2021). Specifically, we conduct the experiments on CIFAR-10 (Krizhevsky et al., 2009), with initial labeled size  $|\mathcal{L}_{init}^{CIFAR-10}| = 100$  (randomly sampled from the train split), per-episode budget  $B_{CIFAR-10} = 1$ , and number of acquisition episode  $E = 25$ . We compare the updated models performance (accuracy) on the test split of CIFAR-10. Different from the experiments in §4, we do not apply any AL algorithm when acquiring the sample in each round. Instead, we randomly choose  $B$  sample in each acquisition round from the unlabeled set and then update the models through both methods with the same selected sample.

To access the difference between models updated with our influence function-based method and single backpropagation, we compute the mean squared error (MSE) between the performance of each model and the model updated by conventional full training, which is defined in Eq. (3).

Based on the result showed in Fig. 4a, we see that the proposed method provides more accurate (smaller mean and median) and more robust (smaller std.) model approximations than single backpropagation, contributing to the performance gain we observe in §4.

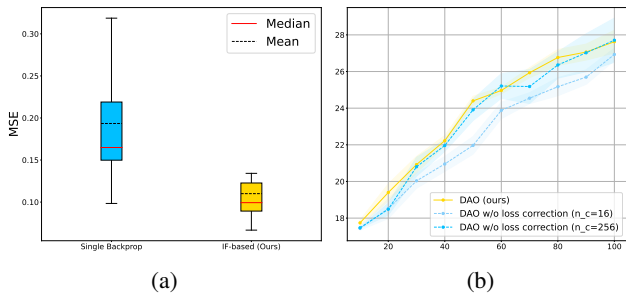


Figure 4. *Left*: MSE of the predictions accuracy on the test split of CIFAR-10 between models updated by single backpropagation, influence function, and the fully trained model. *Right*: Ablation results where the proposed loss estimation is replaced by the random sampling estimation defined in §5.2.

## 5.2 Bias Correction vs. Random Sampling

Next, we conduct ablation studies on replacing the proposed loss estimation (§3.4) with the average loss of randomly sampled data points. More specifically, we replace the estimated loss  $s_i$  from averaging the corrected loss (Eq. (10)) of the acquired samples via an alternative acquisition criteria (Eq. (13)) with averaging losses of the samples acquired uniformly, i.e., at round  $t$ , we have  $s_i^{\text{random}} = \frac{1}{M_{\text{random}}} \sum_{m=1}^{M_{\text{random}}} \ell(\mathbf{x}_{t,m}; f_t)$  where  $\mathbf{x}_{t,m} \sim U(1, |\mathcal{U}_{t,i}|)$ . We choose two  $M_{\text{random}} = 16$  and 256, where former provides a direct comparison with our proposed loss estimation approach, and latter represents a brute-force solution that works relatively well but is often infeasible in practice due to intensive running time.

The results are showed in Fig. 4b. We see that the proposed method performs even better than the conventional random-sampling loss estimation with large sampling size, while computationally being only 1/8 of the run time. Additionally, the variance of our method is much smaller, indicating more robust loss estimation, which translates to more robust acquisition performance.

## 6 Related Work

**Active learning.** AL has gained a lot of attraction in recent years, with its goal to achieve better model performance with fewer training data (Freund et al., 1997; Graepel & Herbrich, 2000; Schohn & Cohn, 2000; Fine et al., 2002; Hoi et al., 2006; Guillory & Bilmes, 2011; Yang & Carbonell, 2013; Chen et al., 2021). There have been different selection criteria including uncertainty (Lewis, 1995), query-by-committee (Seung et al., 1992), version space (Mitchell, 1982) and information-theoretic heuristics (Hoi et al., 2006). The uncertainty-based selection criteria is arguably the most popular, which includes methods like least confidence (Lewis, 1995), minimum margin (Scheffer et al., 2001), and maximum entropy (Settles, 2009). At their core, these methods select points where

the classifier is least certain. However, uncertainty-based methods can be biased towards the current learner. Query-by-committee and version space (Seung et al., 1992; Abe, 1998; Mitchell, 1982), on the other hand, keep a pool of models, and then select samples that maximize the disagreements between them. Information-theoretic methods (Hoi et al., 2006; Barz et al., 2018) typically utilizes mutual information as criteria.

**EER-based acquisition criterion.** Alternatively, EER was proposed to select new training examples that result in the lowest expected error on future test examples, which directly optimizes the metric by which the model will be evaluated (Roy & McCallum, 2001). In essence, EER employs sample selection based on the estimated impact of adding a new data point to the training set, rather than evaluating performance against a separate validation set, meaning that it does not inherently require a validation hold-out set. However, its necessity to retrain the model for every possible candidate sample and every possible label renders its cost intractable in the context of deep neural networks (Budd et al., 2021; Škoda et al., 2020; Ding et al., 2023). More recent EER-based AL algorithms (Killamsetty et al., 2021; Musmann et al., 2022) focus on addressing this efficiency concern. However, these methods rely on a small set of validation data to be used for the evaluation of the expected loss reduction, which is not ideal for the low-budget AL settings. In this paper, we present DAO, a novel AL algorithm that improves upon EER through optimizations on both model updates as well as loss estimation, efficiently and effectively broadening the applicability of EER-based algorithm.

## 7 Conclusions and Future Work

In this paper, we introduced Direct Acquisition Optimization (DAO), a novel algorithm designed to optimize sample selections in low-budget settings. DAO hinges on the utilization of influence functions for model parameter updates and a separate acquisition strategy to mitigate bias in loss estimation, represents a significant optimization of the EER method and its modern follow-ups. Through empirical studies, DAO has demonstrated superior performance in low-budget settings, outperforming existing state-of-the-art methods by a significant margin across seven datasets.

Looking ahead, several promising directions for future research can be explored. First, further exploration into the scalability of DAO in larger and more complex datasets will be crucial. Second, an in-depth investigation into the influence function’s behavior in different model architectures could yield insights that further refine and enhance the DAO framework. And finally, integrating DAO with other machine learning paradigms, such as unsupervised and semi-supervised learning, could lead to the development of more robust and versatile active learning frameworks.



## Acknowledgement

This work was supported in part by NSF RI:2313130, NSF 2037026, the Data Science Institute’s AI+Science Research Initiative, and the Research Computing Center at the University of Chicago. Any opinions, findings, conclusions, or recommendations expressed in this material are those of the authors and do not necessarily reflect the views of any funding agencies.

## References

- Abe, N. Query learning strategies using boosting and bagging. In *International Conference on Machine Learning, 1998*, pp. 1–9, 1998.
- Adadi, A. A survey on data-efficient algorithms in big data era. *Journal of Big Data*, 8(1):24, 2021.
- Agarwal, N., Bullins, B., and Hazan, E. Second-order stochastic optimization for machine learning in linear time. *The Journal of Machine Learning Research*, 18(1): 4148–4187, 2017.
- Ash, J. T., Zhang, C., Krishnamurthy, A., Langford, J., and Agarwal, A. Deep batch active learning by diverse, uncertain gradient lower bounds. *arXiv preprint arXiv:1906.03671*, 2019.
- Barz, B., Käding, C., and Denzler, J. Information-theoretic active learning for content-based image retrieval. In *German Conference on Pattern Recognition*, pp. 650–666. Springer, 2018.
- Budd, S., Robinson, E. C., and Kainz, B. A survey on active learning and human-in-the-loop deep learning for medical image analysis. *Medical Image Analysis*, 71: 102062, 2021.
- Chandra, A. L., Desai, S. V., Devaguptapu, C., and Balasubramanian, V. N. On initial pools for deep active learning. In *NeurIPS 2020 Workshop on Pre-registration in Machine Learning*, pp. 14–32. PMLR, 2021.
- Chen, S., Kahla, M., Jia, R., and Qi, G.-J. Knowledge-enriched distributional model inversion attacks. In *Proceedings of the IEEE/CVF international conference on computer vision*, pp. 16178–16187, 2021.
- Coates, A., Ng, A., and Lee, H. An analysis of single-layer networks in unsupervised feature learning. In *Proceedings of the fourteenth international conference on artificial intelligence and statistics*, pp. 215–223. JMLR Workshop and Conference Proceedings, 2011.
- Cook, R. D. and Weisberg, S. Residuals and influence in regression, 1982.
- Deng, J., Dong, W., Socher, R., Li, L.-J., Li, K., and Fei-Fei, L. Imagenet: A large-scale hierarchical image database. In *2009 IEEE conference on computer vision and pattern recognition*, pp. 248–255. Ieee, 2009.
- Ding, Y., Martín-Guerrero, J. D., Vives-Gilabert, Y., and Chen, X. Active learning in physics: From 101, to progress, and perspective. *Advanced Quantum Technologies*, pp. 2300208, 2023.
- Farquhar, S., Gal, Y., and Rainforth, T. On statistical bias in active learning: How and when to fix it. *arXiv preprint arXiv:2101.11665*, 2021.
- Fine, S., Gilad-Bachrach, R., and Shamir, E. Query by committee, linear separation and random walks. *Theoretical Computer Science*, 284(1):25–51, 2002.
- Freund, Y., Seung, H. S., Shamir, E., and Tishby, N. Selective sampling using the query by committee algorithm. *Machine learning*, 28:133–168, 1997.
- Fu, W., Wang, M., Hao, S., and Wu, X. Scalable active learning by approximated error reduction. In *Proceedings of the 24th ACM SIGKDD international conference on knowledge discovery & data mining*, pp. 1396–1405, 2018.
- Gal, Y., Islam, R., and Ghahramani, Z. Deep bayesian active learning with image data. In *International conference on machine learning*, pp. 1183–1192. PMLR, 2017.
- Graepel, T. and Herbrich, R. The kernel gibbs sampler. *Advances in Neural Information Processing Systems*, 13, 2000.
- Guillory, A. and Bilmes, J. A. Online submodular set cover, ranking, and repeated active learning. *Advances in neural information processing systems*, 24, 2011.
- Hacohen, G., Dekel, A., and Weinshall, D. Active learning on a budget: Opposite strategies suit high and low budgets. *arXiv preprint arXiv:2202.02794*, 2022.
- He, K., Zhang, X., Ren, S., and Sun, J. Deep residual learning for image recognition. In *Proceedings of the IEEE conference on computer vision and pattern recognition*, pp. 770–778, 2016.
- Hoi, S. C., Jin, R., Zhu, J., and Lyu, M. R. Batch mode active learning and its application to medical image classification. In *Proceedings of the 23rd international conference on Machine learning*, pp. 417–424, 2006.
- Huang, K.-H. Deepal: Deep active learning in python. *arXiv preprint arXiv:2111.15258*, 2021.

- Huijben, I. A., Kool, W., Paulus, M. B., and Van Sloun, R. J. A review of the gumbel-max trick and its extensions for discrete stochasticity in machine learning. *IEEE Transactions on Pattern Analysis and Machine Intelligence*, 45(2):1353–1371, 2022.
- Killamsetty, K., Sivasubramanian, D., Ramakrishnan, G., and Iyer, R. Glister: Generalization based data subset selection for efficient and robust learning. In *Proceedings of the AAAI Conference on Artificial Intelligence*, volume 35, pp. 8110–8118, 2021.
- Kirsch, A., Farquhar, S., Atighehchian, P., Jesson, A., Branchaud-Charron, F., and Gal, Y. Stochastic batch acquisition for deep active learning. *arXiv preprint arXiv:2106.12059*, 2021.
- Koh, P. W. and Liang, P. Understanding black-box predictions via influence functions. In *International conference on machine learning*, pp. 1885–1894. PMLR, 2017.
- Kossen, J., Farquhar, S., Gal, Y., and Rainforth, T. Active testing: Sample-efficient model evaluation. In *International Conference on Machine Learning*, pp. 5753–5763. PMLR, 2021.
- Krause, J., Stark, M., Deng, J., and Fei-Fei, L. 3d object representations for fine-grained categorization. In *Proceedings of the IEEE international conference on computer vision workshops*, pp. 554–561, 2013.
- Krizhevsky, A., Hinton, G., et al. Learning multiple layers of features from tiny images. 2009.
- LeCun, Y., Bottou, L., Bengio, Y., and Haffner, P. Gradient-based learning applied to document recognition. *Proceedings of the IEEE*, 86(11):2278–2324, 1998.
- Lewis, D. D. A sequential algorithm for training text classifiers: Corrigendum and additional data. In *Acm Sigir Forum*, volume 29, pp. 13–19. ACM New York, NY, USA, 1995.
- Ling, R. F. Residuals and influence in regression, 1984.
- Liu, Z., Ding, H., Zhong, H., Li, W., Dai, J., and He, C. Influence selection for active learning. In *Proceedings of the IEEE/CVF International Conference on Computer Vision*, pp. 9274–9283, 2021.
- Martens, J. et al. Deep learning via hessian-free optimization. In *ICML*, volume 27, pp. 735–742, 2010.
- Mitchell, T. M. Generalization as search. *Artificial intelligence*, 18(2):203–226, 1982.
- Mittal, S., Tatarchenko, M., Çiçek, Ö., and Brox, T. Parting with illusions about deep active learning. *arXiv preprint arXiv:1912.05361*, 2019.
- Mussmann, S., Reislter, J., Tsai, D., Mousavi, E., O’Brien, S., and Goldszmidt, M. Active learning with expected error reduction. *arXiv preprint arXiv:2211.09283*, 2022.
- Ren, P., Xiao, Y., Chang, X., Huang, P.-Y., Li, Z., Gupta, B. B., Chen, X., and Wang, X. A survey of deep active learning. *ACM computing surveys (CSUR)*, 54(9):1–40, 2021.
- Roy, N. and McCallum, A. Toward optimal active learning through monte carlo estimation of error reduction. *ICML, Williamstown*, 2:441–448, 2001.
- Scheffer, T., Decomain, C., and Wrobel, S. Active hidden markov models for information extraction. In *International symposium on intelligent data analysis*, pp. 309–318. Springer, 2001.
- Schohn, G. and Cohn, D. Less is more: Active learning with support vector machines. In *ICML*, volume 2, pp. 6, 2000.
- Sener, O. and Savarese, S. Active learning for convolutional neural networks: A core-set approach. *arXiv preprint arXiv:1708.00489*, 2017.
- Sermanet, P., Chintala, S., and LeCun, Y. Convolutional neural networks applied to house numbers digit classification. In *Proceedings of the 21st international conference on pattern recognition (ICPR2012)*, pp. 3288–3291. IEEE, 2012.
- Settles, B. Active learning literature survey. 2009.
- Seung, H. S., Opper, M., and Sompolinsky, H. Query by committee. In *Proceedings of the fifth annual workshop on Computational learning theory*, pp. 287–294, 1992.
- Simonyan, K. and Zisserman, A. Very deep convolutional networks for large-scale image recognition. *arXiv preprint arXiv:1409.1556*, 2014.
- Sinha, S., Ebrahimi, S., and Darrell, T. Variational adversarial active learning. In *Proceedings of the IEEE/CVF International Conference on Computer Vision*, pp. 5972–5981, 2019.
- Škoda, P., Podsztavek, O., and Tvrdík, P. Active deep learning method for the discovery of objects of interest in large spectroscopic surveys. *arXiv preprint arXiv:2009.03219*, 2020.
- Tong, S. and Koller, D. Support vector machine active learning with applications to text classification. *Journal of machine learning research*, 2(Nov):45–66, 2001.
- van der Ploeg, T., Austin, P. C., and Steyerberg, E. W. Modern modelling techniques are data hungry: a simulation study for predicting dichotomous endpoints. *BMC medical research methodology*, 14(1):1–13, 2014.

- Xiao, H., Rasul, K., and Vollgraf, R. Fashion-mnist: a novel image dataset for benchmarking machine learning algorithms. *arXiv preprint arXiv:1708.07747*, 2017.
- Yang, L. and Carbonell, J. Buy-in-bulk active learning. *Advances in neural information processing systems*, 26, 2013.
- Zhan, X., Wang, Q., Huang, K.-h., Xiong, H., Dou, D., and Chan, A. B. A comparative survey of deep active learning. *arXiv preprint arXiv:2203.13450*, 2022.
- Zhu, Y., Lin, J., He, S., Wang, B., Guan, Z., Liu, H., and Cai, D. Addressing the item cold-start problem by attribute-driven active learning. *IEEE Transactions on Knowledge and Data Engineering*, 32(4):631–644, 2019.

## A Appendix

### A.1 More Empirical Analysis Results

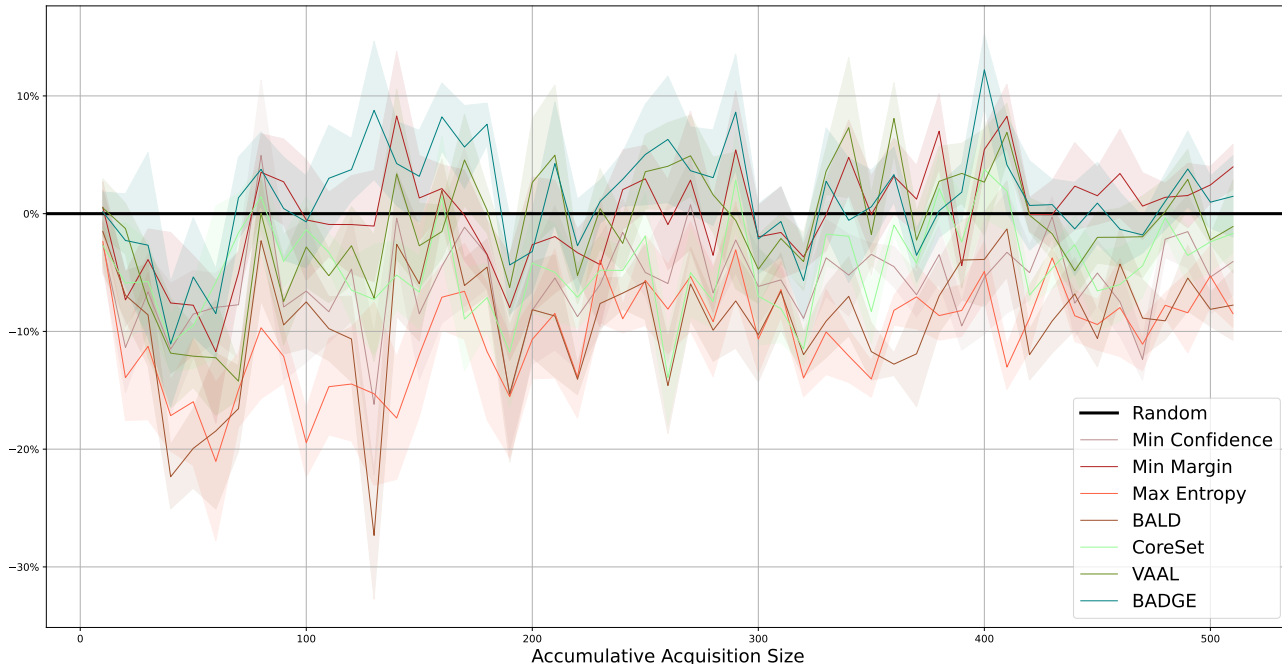


Figure 5. Relative performance between existing popular AL methods and random acquisition. horizontal axis represents the accumulative size of the labeled set, while vertical axis indicates relative performance in percentage.

### A.2 Experiments on Different Stochastic Batch Acquisitions

In this section, we further study the performance of DAO when no batch sampling strategy or other sampling strategy is used and compare the results with existing popular AL algorithms. The results are showed in Fig. 6. For all experiments, we used the same low-budget setting as discussed in §4.3.

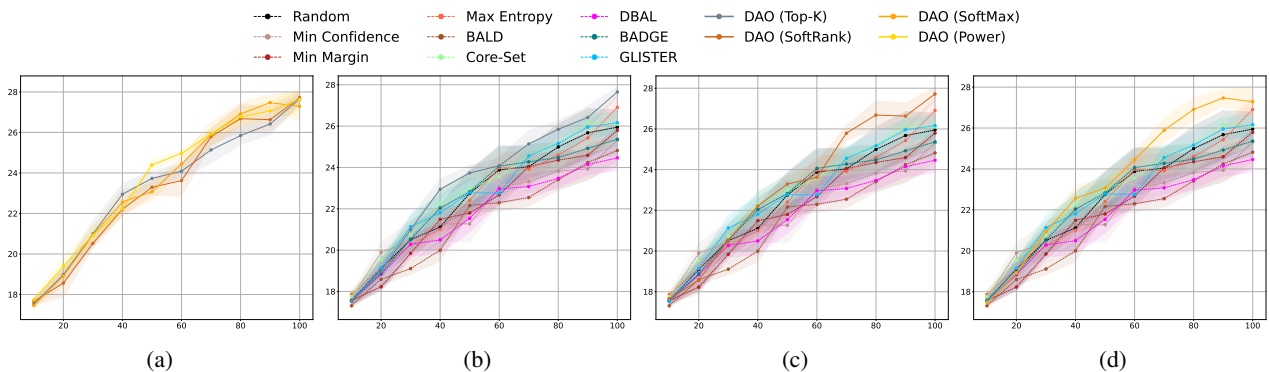


Figure 6. CIFAR-10 experiment results on (a): DAO without batch acquisition strategy (using naive top-k selection) and with other sampling strategies (softmax and softrank, as discussed in §3.5); (b): DAO without sampling (top-k) vs. existing AL algorithms; (c): DAO with softrank sampling vs. existing AL algorithms; (d): DAO with softmax sampling vs. existing AL algorithms; In all subplots, horizontal axis represents the accumulative size of the labeled set, while vertical axis indicates classification accuracy.